Cloud and microphysical schemes in ARPEGE and AROME models

Yann Seity, Christine Lac, Francois Bouyssel, Sebastien Riette, and Yves Bouteloup

Météo-France, CNRM/GAME, Toulouse, France
Contact: yann.seity@meteo.fr

ABSTRACT

Physics of AROME and ARPEGE models used at Météo-France are closer and closer, but nevertheless their microphysics and cloud schemes exhibit some differences. Both consider a 1-moment microphysical scheme, but AROME uses one more hydrometeor category, the graupel, which is particularly important in convective events. In AROME, a hail diagnostic has been prefered to an additional prognostic variable, based on vertically integrated graupel content. The sedimentation scheme is common between both models, but with one more term required in ARPEGE considering the microphysical processes occuring during the fall of the longer time step. The PDF used in the subgrid cloud schemes are also different. In addition to other aspects linked with mesoscale data assimilation, model grid and temporal sampling, these differences help AROME to have better rain forecasts than ARPEGE, especially in convective situations. Some developments are performed in Meso-NH in order to prepare the implementation of more advanced microphysical schemes in AROME.

1 Introduction

With the increase of computing power, horizontal and vertical resolutions of NWP systems are frequently improved. Cloud representation in NWP models is a crucial issue, due to many interactions with dynamics, radiation, surface energy budget and aerosols. Despite the fact that less subgrid scale parameterization of cloud effect may be necessary as horizontal and vertical resolution increase, consideration of subgrid cloud variability remains important at kilometric resolutions especially for high non linear processes like precipitation. Another aspect is that operational cloud resolving models, which are limited area models, usually use 1-moment microphysics schemes, but 2-moment microphysics are becoming more and more the standard in research. In this context, we will present in the following sections the current status of cloud and microphysics schemes in Météo-France NWP systems, and some research work preparing their future udpate. Section 2 presents the AROME and ARPEGE NWP systems. Section 3 explains how water is represented in these systems. Section 4 details sub-grid cloud processes whereas section 5 deals with microphysics schemes. The last section provides some scores and test cases.

2 Presentation of ARPEGE and AROME

Over mainland France, two operational numerical weather prediction systems are operated by Météo-France: the global model ARPEGE and the Limited Area Model AROME [Seity et al., 2010]. ARPEGE forecasts run with a time step of 9 minutes on a stretched grid allowing a 10 km resolution grid mesh over France and around 60km over antipodes. The vertical discretisation is performed on 70 levels, with the lowest one at 17.5m. ARPEGE is initialized by a 4D-Var data assimilation scheme running at lower resolution on a regular grid (T107 ($\tilde{1}$80km) and T323 ($\tilde{6}$0km)).

With its 2.5 km horizontal grid mesh, AROME (Applications of Research to Operations at MesoscalE) is a non-hydrostatic model devoted to meso-scale phenomena prediction. The model grid contains 750x720 points and 60 vertical levels (the lowest one being at 10 meters). A time step of 1 minute is used. The model has been built upon the ALADIN-NH dynamical core (bi-Fourier spectral limited-aera model with a semi-implicit, semi-lagrangian timestep solver, and Laprise-type compressible dynamical equation in terrain-following hybrid mass coordinates). It comprises a 3-hourly Rapid Update Cycle in a 3DVar data assimilation system which uses meso-scale observations (such as radar reflectivities [Caumont et al., 2009, Wattrelot et al., 2008] and Doppler winds [Montmerle and Faccani, 2009] in addition to other kind of observations used also in ARPEGE. Its atmospheric physics, which is 1D, comes from Meso-NH research model [Lafore et al., 1998], including turbulence, shallow convection, microphysical and cloud schemes. But nevertheless, AROME and ARPEGE physics are closer and closer. Indeed, even if time step and horizontal resolution are different (from dt=1 min, dx=2.5 km in AROME to dt=1800s and dx=180km in ARPEGE 4D var), they use the same turbulence scheme with prognostic TKE [Cuxart et al., 2000] and [Bougeault and Lacarrere, 1989] mixing length, same radiation schemes (RRTM [Mlawer et al., 1997] for long-wave and Fouquart-Morcrette [Fouquart and Bonnel, 1980] for short wave (SW). AROME shallow convection scheme [Pergaud et al., 2009] is currently tested in ARPEGE and the one of ARPEGE [Bechtold et al., 2001] is also available in AROME. According to its meso-scale horizontal resolution, some physical parameterizations required in ARPEGE does not exist in AROME (deep convection and orographic drag).The remaining main differences are located in the microphysics and cloud schemes which will be detailed in the next sections.

In this context, AROME and Meso-NH present a complementarity to develop and improve physical parameterisations (Meso-NH is based on eulerian explicit dynamics), as Meso-NH uses its own LES to develop parametrization that can be validated in AROME.

3 The water representation

In addition to water vapor (content $\overline{r}_v$), AROME-operational set of prognostic variables contains 5 water condensates : cloud droplets $\overline{r}_c$, rain $\overline{r}_r$, ice crystals $\overline{r}_i$, snow $\overline{r}_s$, graupel $\overline{r}_g$ and ARPEGE only 4 (liquid clouds $\overline{r}_c$, rain $\overline{r}_r$, icy clouds $\overline{r}_i$ and snow $\overline{r}_s$). They are advected by the Semi-Lagrangian (SL) scheme but they also react with the "dynamics" through inertia and gravity terms in the momentum equation and their thermal inertia in the thermodynamic equation.

The first step of AROME physics is the adjustment to saturation. In ARPEGE, it is done just before radiation, after shallow convection and turbulence. This step ensures the thermodynamic equilibrium between water species and temperature before calling physical parameterizations. The adjusted variables are then used in the rest of the physics. This process of adjustment to saturation is supposed to be significantly faster than processes of the precipitating microphysics described in section 5. This step also diagnoses cloud fraction (CF) (which will be an input to the radiation scheme called just after) using information from a subgrid condensation scheme. This subgrid scheme will use input information from turbulence scheme and convection schemes (shallow for AROME, Shallow+Deep for ARPEGE, cf section 4 for more details).

In the SW radiation scheme, for $\overline{r}_c$, optical properties are derived from [Morcrette and Fouquart, 1986] and the effective radius is diagnosed from [Martin et al., 1994] formulation. For $\overline{r}_i$, optical properties come from [Ebert and Curry, 1992], and the effective radius is diagnosed from temperature using a revision of the [Ou and Liou, 1995] formulation. Precipitating species (rain, snow and graupel) are not used yet in radiation. Cloud cover is computed in each column using the maximum cover value for sets of adjacent cloudy layers, and a random overlap assumption between cloudy layers separated by clear layers. In AROME, the microphysics scheme works on same cloud variables as those seen by radiation. It is not the case in ARPEGE as radiation scheme uses clouds from deep convection scheme, whereas

microphysics does not. Indeed a simple microphysics scheme is embedded in the deep convection scheme (cf section 5.1 for more details).

4 The subgrid cloud processes

4.1 Subgrid clouds in ARPEGE

The parameterization of clouds and precipitations in ARPEGE physics relies on a prognostic representation of four condensate water species (cloud droplets, ice cristal, rain, snow) for "resolved" and shallow convective clouds and a diagnostic representation for deep convective clouds.

A statistical cloud scheme using a triangular symetric probability density function (PDF) for subgrid fluctuations of the departure to a local saturation inside the grid box [Smith, 1990] provides cloudiness and cloud water contents (liquid and solid) for "resolved" clouds assuming cloud condensation and evaporation being instantaneous and reversibles. The width of the PDF is defined by a critical relative humidity which decreases with model level height and horizontal resolution. The partition between liquid and ice clouds is function of temperature.

Moist shallow convection is represented with a mass flux scheme with a CAPE closure [Bechtold et al., 2001]. Cloud condensate rates (liquid and solid) are used to diagnose cloudiness and cloud water contents of shallow convective clouds.

"Resolved" and shallow convective clouds are combined with a maximum overlap assumption to provide an updated state of cloudiness and prognostic cloud liquid and ice water contents.

Deep convection is described with a mass-flux scheme based on a moisture convergence closure for triggering and intensity [Bougeault, 1985]. The rate of condensation is used to diagnose cloudiness and cloud water contents of deep convective clouds. "Resolved", shallow and deep convective clouds macroscale properties (cloudiness, cloud water contents) are combined assuming a maximum random overlap asumption to compute cloud/radiation interactions.

4.2 Subgrid clouds in AROME

The statistical cloud scheme from AROME comes from MESO-NH [Bougeault, 1982], [Bechtold et al., 1995], and is based on the computation of the variance of the departure to a local saturation inside the grid box. If the grid box is saturated with respect to the mean variables ($\overline{r}_{np} > r_{sat}(\overline{T})$, with r_{np} the total non precipitating mixing ratio) and if the variance is small, the cloud parameters (cloud contents and cloud fraction) are close to the ones obtained with an "all or nothing" adjustment. If the mean variables are saturated but the variance is high, the cloud parameters are given by a gaussian probability density function (PDF) (the cloud fraction is larger than 0.5 but smaller than one). If the mean variables do not reach saturation, but the variance is relatively high, the cloud fraction (smaller than 0.5) and the cloud condensate content are given by a combination between a gaussian and a skewed exponential PDF (Fig. 1).

Subgrid variability from the eddy diffusivity turbulent scheme [Cuxart et al., 2000] relies on the departure to saturation σ_{turb} which is computed from the variances of the liquid potential temperature $\overline{\theta_l'^2}$ and of the total non precipitationg water $\overline{r_{np}'^2}$.

To take into account the subgrid variability from the shallow convection scheme [Pergaud et al., 2009], two options are possible :

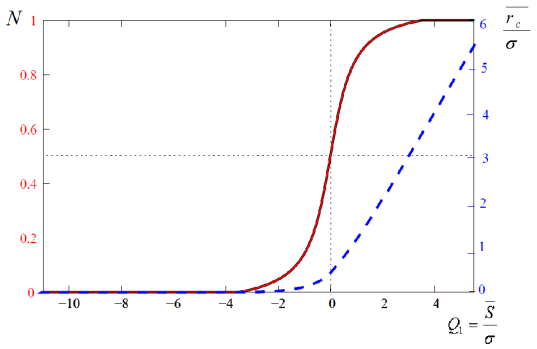

Figure 1: Cloud fraction (solid line) and normalised cloud mixing ratio (dashed line) as a function of the normalised mean departure to saturation $\overline{s} = \overline{r}_{np} - r_{sat}$ for the statistical cloud scheme of MESO-NH. σ^2 is the variance of the departure to saturation which is estimated in the subgrid mixing parametrization (turbulence and possibly shallow convection with the STAT method).

- A similar approach of variance σ_{conv} can be used as the variances of θ_l and r_{np} are computed from the shallow convection parametrization (called *STAT* method). σ_{turb} and σ_{conv} are added and applied to the PDFs presented on Fig. 1.
- The cloud profiles of the shallow updrafts are used more directly instead of the variance of the convective part. The cloud fraction and r_c and r_i are diagnosed from the updraft fraction α_u as :

  $$\alpha_u = M_u/(\rho w_u)$$

  where M_u and w_u are the updraft mass flux and vertical velocity respectively. The convective cloud parameters are then combined with the cloud parameters resulting from the statistical adjustment which uses only the eddy turbulent variance σ_{turb} (called *DIRECT* method).

The *DIRECT* method presents the advantage to take into account the spatial dimension of the updraft, on the contrary to the *STAT* method, that consequently tends to overestimate the cloud coverages. The *DIRECT* method has been chosen for the operational version of AROME. The figure 2b. and c. illustrates differences between both methods for the case of 9 April 2010 at 12UTC over Netherlands.

Apart from turbulence and convection, there can be other sources of variance like gravity waves, in particular with stable conditions when turbulent and convective contributions are too weak to produce clouds. Following [Rooy et al., 2010], a variance term proportional to the saturation total water specific humidity is added. In this way, it gets the characteristics of a RH-scheme, where cloud cover is simply a function of the relative humidity. This added term has shown significative improvements especially for some winter situations, as illustrated on Fig. 3 for 10 January 2010.

4.3 Towards a double gaussian PDF

In order to characterize the distributions of the horizontal subgrid cloud variability, a statistical analysis of large-eddy simulations (LES) obtained for warm BL clouds has been carried out with Meso-NH in [Perraud et al., 2011]. For the ARM cumulus case for instance, the shape of the LES saturation deficit distributions are illustrated on Fig. 4 for various levels from the cloud base to the cloud top. The PDF are non-symmetric bell shaped curves with a positive or negative skewness. A second mode is clearly seen for high values of supersaturation in the lower part of the cloud layer. Higher in the cloud layer, the second mode vanishes into a long flat tail. A conditional sampling of LES data according to [F. Couvreux and Rio, 2010], carried on in order to characterize the processes of both modes,

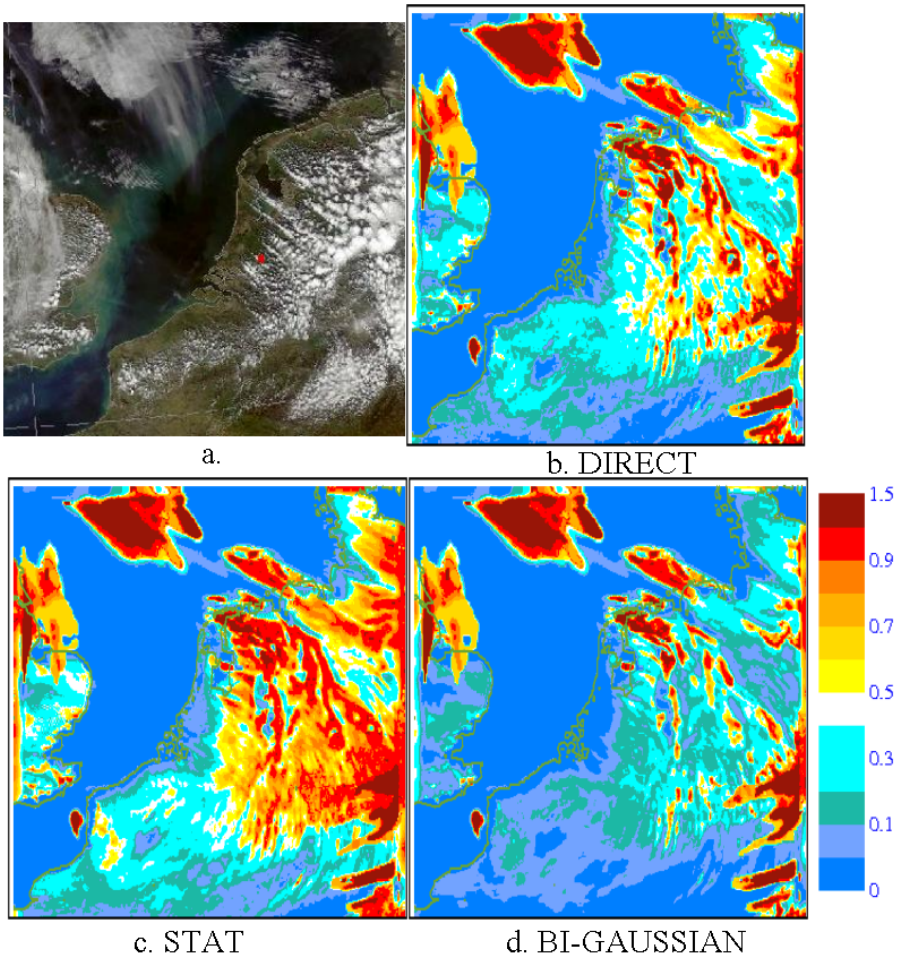

Figure 2: a. Visible satellite image from MSG the 9 April 2010 at 12:00 UTC. b, c and d : Predicted cloud fraction with AROME with the DIRECT (b), STAT (c) and BI − GAUSSIAN (d) methods.

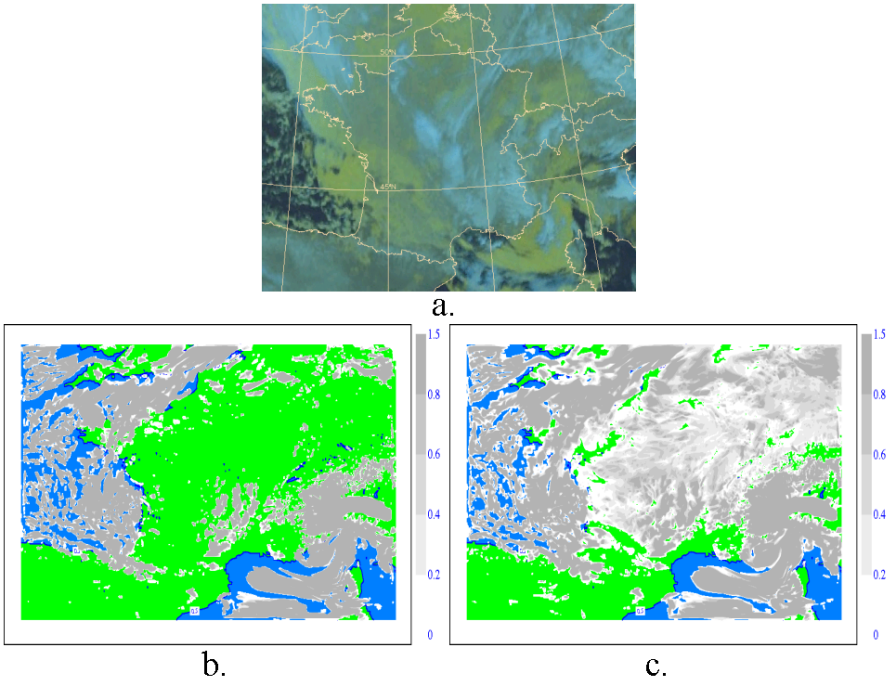

Figure 3: a. Water vapor satellite image from MSG2-MET9 the 10 January 2010 at 6:00 UTC. b. Predicted cloud fraction with AROME without [Rooy et al., 2010] added term. c. Predicted cloud fraction with AROME with [Rooy et al., 2010] term.

has shown that the second mode is clearly associated to the updrafts (Fig. 5). Unimodal PDFs are not sufficient to correctly fit the LES distributions, especially the long tail that appears for cumulus clouds. On the contrary, double Gaussian distributions are more appropriate, as already proposed by [Larson et al., 2001a, Larson et al., 2001b] or [Golaz et al., 2002a, Golaz et al., 2002b], as they improve the description of sparse subgrid clouds such as shallow cumuli and fractional stratocumuli. This double Gaussian distribution is equal to a linear combination of two simple Gaussian distributions, where the parameters of the first simple Gaussian are given by the turbulence scheme, and the parameters of the second one by the shallow convection scheme, by analogy with [Lenderink and Siebesma, 2000]. The figure 2 illustrates the result with the double gaussian PDF (noted $BI-GAUSSIAN$). But it is not obvious to get a subjective preference between the methods. An objective evaluation based on soundings and satellite products is on going (Riette, 2013, in preparation).

4.4 Towards subgrid rains in AROME

Observations have shown that precipitation embryos in warm clouds are formed when the mean volume droplet radius of the droplet size distribution reaches a threshold of $10-12\ \mu m$. The onset of precipitation is thus particularly sensitive to the likelihood of a few droplets (a few per liter) reaching this threshold radius, and this depends on the local values of liquid water content and droplet number concentration. An objective has been to represent subgrid rain in AROME, especially for cumuli and stratocumuli, even if objective scores do not reveal a systematic failure for light rains (cf part.6). In [Turner et al., 2012], a method has been developed in Meso-NH to represent the gradual transition from non-precipitating to fully precipitating model grids, based on the analogy with the statistical representation of subgrid cloud schemes : the variability of the cloud water content in the cloud fraction of a model grid is represented by a PDF and precipitation is initiated in the subcloud fraction where the

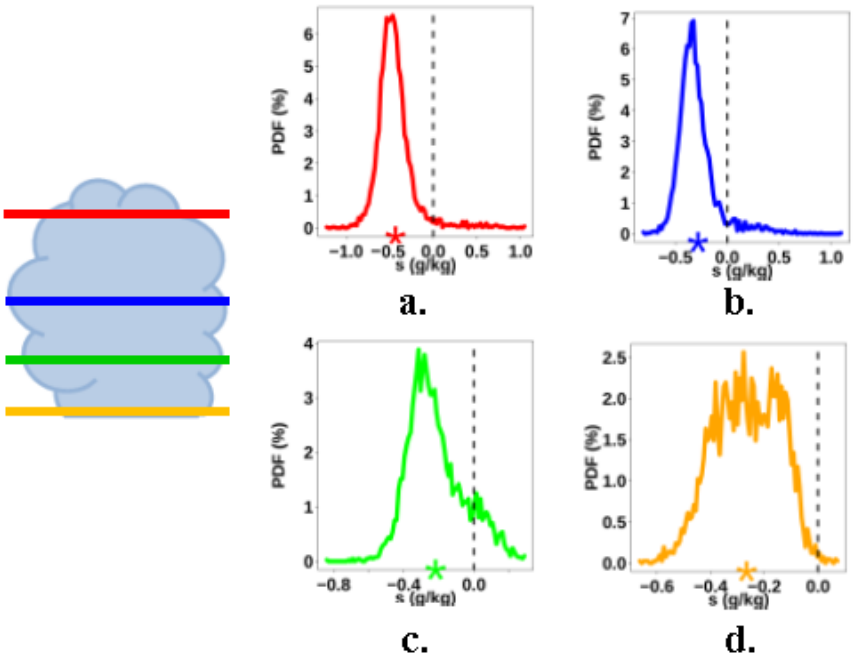

Figure 4: From [Perraud et al., 2011] : LES distribution of departure to saturation s inside the cloud layer for the ARM case. a corresponds to the top of the cloud layer to d for the base. The vertical dashed line represents saturation ($s = 0$) and the star on the x-axis the mean value of s.

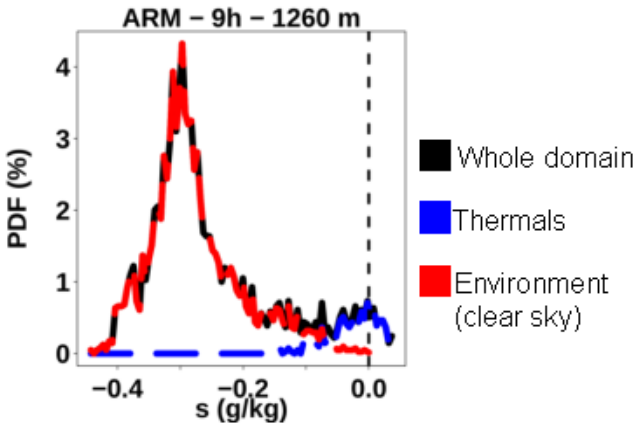

Figure 5: From [Perraud et al., 2011] : LES distribution of departure to saturation s for the ARM case at a level in the lower part of the cloud layer. The distribution of the whole horizontal domain is in black, the clear sky in red and the ascending cloudy zone in blue. The vertical dashed line represents saturation ($s = 0$).

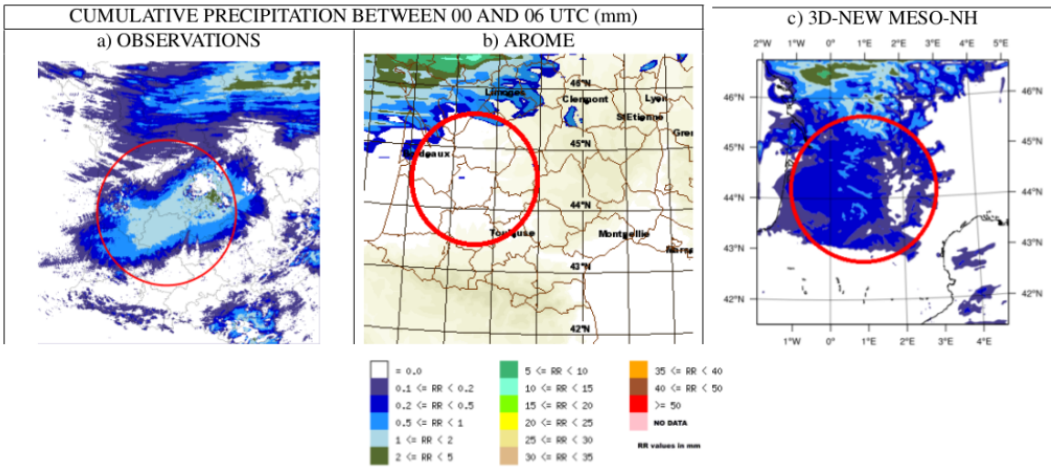

Figure 6: From [Turner et al., 2012] : 6h-cumulated precipitation for 27 March 2009 : (a) Radar observations. (b) : AROME forecast. (c) : Meso-NH prediction with the subgrid rain. (d) : Meso-NH prediction without the subgrid rain.

values of the cloud water content are greater than the autoconversion threshold. The local value of the cloud water content in the cloudy fraction is defined as the ratio of the grid mean value in the model by the cloud fraction (CF), supplied by the cloud scheme. The cloudy fraction is then divided into two parts, in which the local values of the cloud water mixing ratio are respectively lower (CF_L) and higher (CF_H) than the autoconversion threshold of the microphysical scheme. The local value of rain water content corresponds to the ratio of the mean rain content value by the rain fraction (RF) in the model grid. A realistic approach would be to advect the RF like any conservative variable, considering that RF is uniformly distributed over each model grid, but the constraint for AROME is to avoid adding a new prognostic variable into the model. The maximum cloud overlap assumption is chosen for the vertical overlap of RF. The drops collect droplets in the area where RF overlaps cloud fraction, or evaporate when the RF overlaps with clear air depending on the respective values of RF, CF, CF_H and CF_L.

The case of 27 March 2009 illustrates the impact of the subgrid rain scheme (Fig. 6). The BL clouds produce drizzle with low precipitation rates leading to cumulative precipitation of around 1mm for 6 hours (Fig. 6.a). AROME in its operational version simulates the BL clouds but fails to produce drizzle (Fig. 6.b), as well as Meso-NH (Fig. 6.d). The subgrid precipitation corrects the lack of precipitation in Meso-NH (Fig. 6.c). This subgrid rain scheme is currently brought and evaluated in AROME.

5 Microphysics

5.1 In ARPEGE

The microphysical scheme used in ARPEGE is described in [Lopez, 2002] and [Bouteloup et al., 2005]. Four prognostic variables are used to describe specific humidities of cloud droplets, ice cristals, rain and snow. The autoconversion rates of cloud droplets and ice crystals into precipitating drops and snowflakes, are given by the simple formulations of Kessler (1969). For cloud ice, the threshold decreases with temperature, to allow precipitation generation even inside very cold clouds. There is a temperature-dependent ice conversion efficiency [Pruppacher and Klett, 1978]. The collection of cloud liquid water by rain (accretion), the collection of cloud ice by snow (aggregation) and the collection of cloud liquid water by snow (riming) are considered. The collection parameterizations are derived from

the classical continuous collection equation integrated over the Marshall-Palmer exponential particle spectra, and for specified distributions of particle fall speed and mass. Precipitation evaporation is calculated by integrating the equation that describes the evaporation of a single particle over the assumed spectra of particle number, mass, and fall speed. Falling snow is assumed to melt instantaneously as soon as it enters a model layer with temperature above $0C$, provided the associated cooling that does not lead to freezing. A similar representation is done for the freezing of rain.

5.2 In AROME

The microphysical scheme of AROME/MESO-NH has been developed by J.-P.Pinty on the basis of [Caniaux et al., 1994], following the approach of [Lin et al., 1983], that is a three-class ice parameterization coupled to a Kessler's scheme for the warm processes. Hail is also implemented [Lascaux et al., 2006] but is not activated in the current version of AROME : a hail diagnostic is presented in 5.4. It is also a single moment scheme, predicting only the mixing ratio for each species.

The concentration of the precipitating particles (noted i) is parameterized with a total number $N_i = C_i \lambda_i^x$, where λ is the slope parameter of the size distribution, C and x are empirical adjustments drawn from radar observations. For droplets only, the concentration is imposed with $N_c = 300\ cm^{-3}$ over land and $N_c = 100\ cm^{-3}$ over sea. Each category of particle is supposed to be distributed according to a Gamma law :

$$n(D)dD = Ng(D)dD = N\frac{\alpha}{\gamma(\nu)}\lambda^{\alpha\nu}D^{\alpha\nu-1}exp(-(\lambda D)^{\alpha})dD \tag{1}$$

where $g(D)$ is the normalized distribution while ν and α are ajustable parameters. A Marshall-Palmer distribution law is chosen for precipitating species ($\alpha = \nu = 1$) (rain, snow, graupel and hail) and a modal distribution for cloud and ice. Power law relationships are used to relate the mass to the diameter ($m(D) = aD^b$) and the terminal speed velocity to the diameter ($v(D) = cD^d$).

The moments of the Gamma law are expressed according to the classical formulation :

$$\mathrm{M(p)} \quad = \quad \frac{\int_0^\infty D^p n(d)\ dD}{N_i} = \frac{\Gamma(\nu_i + \frac{p}{\alpha_i})}{\lambda_i^p \Gamma(\nu_i)} \tag{2}$$

where $M(p)$ is the p^{th} moment of $g(D)$. The mixing ratio is expressed as $\rho r_i = aNM_i(b)$ where ρ is the air density. Values of α,ν, a, b, c, d, C and x are given for each hydrometeor type from observations.

The microphysical scheme is sketched in Fig. 7. The detailed documentation of the scheme can be obtained at `http://mesonh.aero.obs-mip.fr/mesonh/`. Pristine ice is initiated by homogeneous nucleation (HON) when $T < -35^oC$ or more frequently by heterogeneous nucleation (HEN). These crystals grow by water vapor deposition (DEP) and by the Bergeron-Findeisen effect (BER). The snow (or aggregate) phase is initiated by autoconversion (AUT) of the primary ice crystals. Snow grows by deposition (DEP) of water vapor, by aggregation (AGG) through small crystal collection and by light riming after impaction of cloud droplets (RIM) and of raindrops (ACC). The graupels are produced by the heavy riming of snow (RIM and ACC) or by rain freezing (CFR) when supercooled raindrops come in contact with pristine ice crystals. Conversion of aggregates into graupel by riming is based on the assumption that aggregates exceed a diameter larger than 7 mm. According to the efficiency of their collecting capacity on one hand and to a heat balance on the other, graupels can grow either in a DRY mode or in a WET mode respectively. When temperature is positive, the pristine crystals immediatly melt into cloud droplets (MLT) while the melting snowflakes are converted (CVM) into graupels. Graupel particles progressively melt (MLT) into raindrops as they fall. The other (warm) processes are described by the Kessler scheme: autonversion of cloud droplets (AUT), accretion (ACC) and rain evaporation (EVA). Each condensed water species has a fall speed, including cloud droplets to represent correctly the fog life cycle.

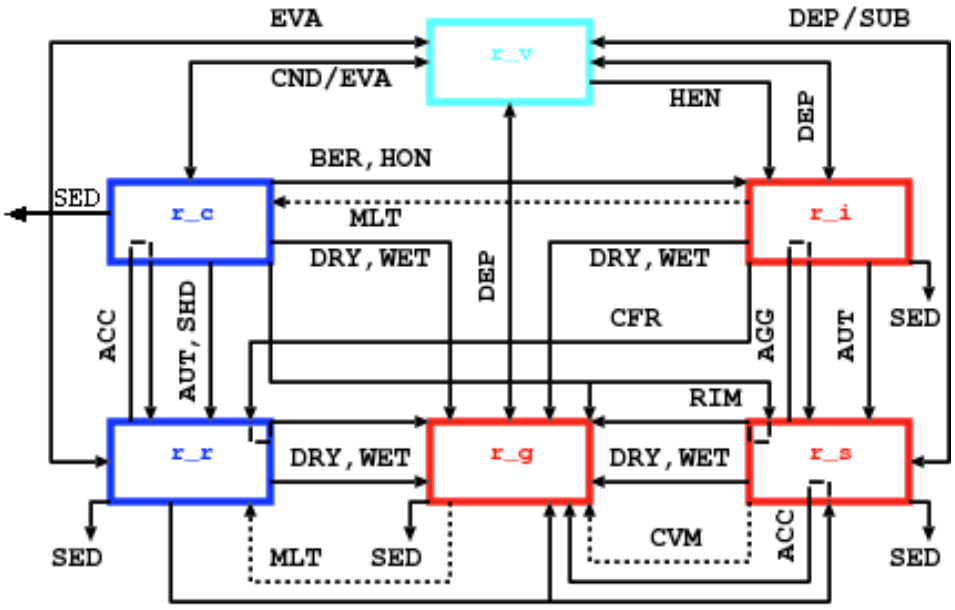

Figure 7: Microphysical processes in the mixed-phase scheme

For the temporal integration, processes are treated explicitely (in terms of tendencies) and independently, but the sequence of the processes gives the availability of the species, as the occurrence of the process is limited by the current state of the guess of the depleted prognostic variable before integration. Some species may be available or not for the next process depending on the chosen order in the sequence of integration.

5.3 Statistical sedimentation

The numerical resolution of the sedimentation equation is replaced by three probabilities of transfer associated with the following three types of precipitation: precipitation present in the layer at the beginning of the time step; precipitation coming from the layer above and crossing the layer under consideration and precipitation produced locally during the time step [Bouteloup et al., 2011]. The main advantage is a near-perfect reproduction of advective (Eulerian or Lagrangian) classical sedimentation schemes at low computation cost.

For each falling hydrometeor, starting from the top layer of the model (where the incoming precipitating flux is zero), a budget is performed on each model layer, to compute the outgoing flux knowing the incoming flux and the hydrometeor content in the considered layer.

In AROME, according to its short time step (1 minute), we neglect the microphysical processes occuring during the fall. The outgoing flux is simply the sum of a fraction (P_1) of the incoming flux (corresponding to the fraction of incoming hydrometeor crossing the model layer in one time step), plus a fraction (P_2) of the hydrometeor contained in the layer. P_1 and P_2 are computed by comparing the hydrometeors fall speed multiplied by the model time step (which corresponds to the travelled vertical distance) to the thickness of the layer. This is the last process of the AROME microphysics scheme.

In ARPEGE, longer time steps force us to take into account microphysical processes during sedimentation. A new term P_3 corresponds to the proportion of $\overline{r_x}$ produced in the layer during δt which leaves the layer during δt. The sedimentation is applied on all species using the fall speeds equation given in part 5.2 in AROME and with constant fall speeds in ARPEGE (5 m/s for rain, 1.5 m/s for snow, 0.02 m/s for cloud and 0.08 m/s for ice).

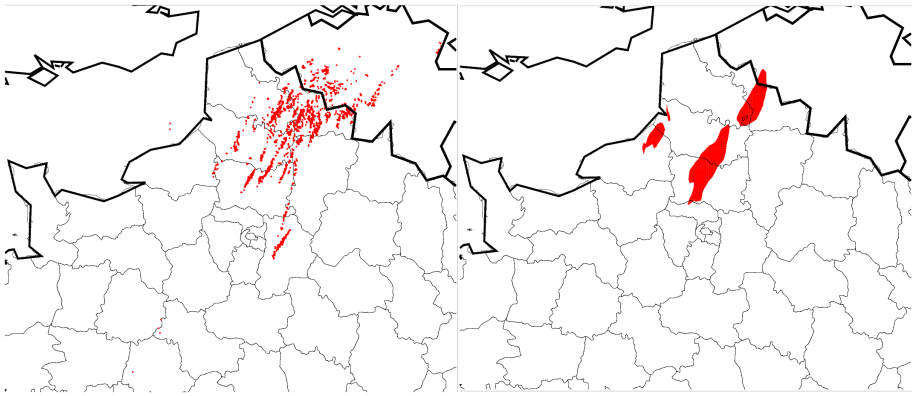

Figure 8: 23 August 2011, between 2 and 8 UTC. Left : hail diagnosed from radar observations, right : hail risk diagnosed by AROME

The general formulation is the following one with $\gamma = 0$ in AROME, $\gamma = 1$ in ARPEGE :

$$F_{n+1} = (1-\gamma\frac{Si_n}{\overline{r_x}+\frac{\delta t}{\rho\delta z}F_n+So_n})(P_1\frac{\rho\overline{r_x}\delta z}{\delta t}+P_2F_n+\gamma P_3\frac{\rho\delta z So_n}{\delta t}) \quad (3)$$

with $P_1 = min(1, w_1\frac{\delta t}{\delta z})$, $P_2 = max(0, 1-\frac{\delta z}{w_2\delta t})$ with $w_2 = F_n\frac{\delta t}{\rho\delta z}$, $P_3 = \frac{P_1+P_2}{2}$, So_n and Si_n are ARPEGE sources and sinks of r_x in layer n, respectively.

5.4 Hail diagnostic in AROME

In the current operational microphysical scheme, hail is part of $\overline{r}_g$. But even in severe summer hailstorms well captured by the model, graupel melts before reaching the ground because its fall speed is too small. Nevertheless, two distinct graupel growth modes are represented : the dry one and the wet one. Physically, it is well known that high density hailstones grow in the wet mode. In order to improve hail forecasts, an option has been developed in the microphysical scheme, which separates hail from graupel with the use of a new prognostic variable $\overline{r_h}$. When graupel is in wet growth mode, a part of $\overline{r_g}$ is converted into $\overline{r_h}$ [Lascaux et al., 2006]. Once created, hail grows by aggregating other microphysics species, falls, and melts. This option has been tested but the results have shown that it was not ready for an operational use. It was too active (small amounts of hail everywhere there was graupel in altitude), and too costly due to the added prognostic variable. Maybe that a more advanced (2-moments for example) microphysics scheme would be required for a correct representation of the physical processes linked with hail. Nevertheless, before such a scheme being used operationally, we develop a hail diagnostic based on information already available in the operational microphysics scheme : it consists every time step, in the computation of the vertically integrated graupel content. The maximum value of this parameter since last model output file is stored in the model files. By using appropriate threshold (16 kg/m^2) this produce, for very low extra cost, an interesting hail risk diagnostic as shown on Fig. 8. This has been implemented in the operational AROME-France since September 2011.

5.5 Towards 2-moment microphysical schemes with Meso-NH

In order to investigate the aerosol-cloud interactions, a 2-moment mixed microphysical scheme has been developped in Meso-NH considering the activation processes of polydisperse populations of CCN and IN, the impaction scavenging by falling raindrops and the transport of the particles [S. Berthet, 2010].

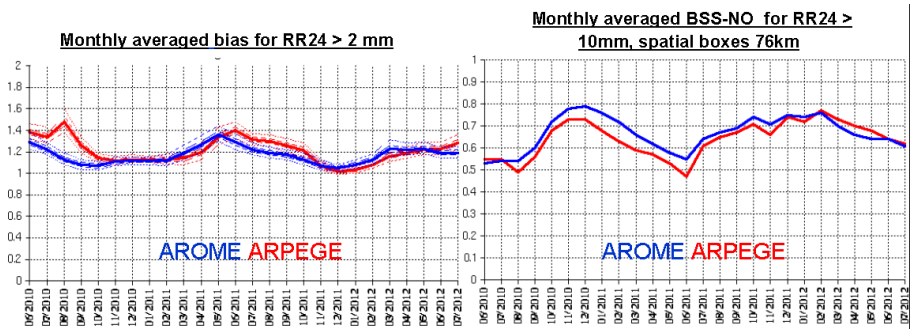

Figure 9: (a) Monthly averaged biases for cumulative daily precipitation (higher than 2mm) from June 2010 to July 2012 for AROME (in blue) and ARPEGE (in red). (b) Monthly averaged Brier Skill Score for cumulative daily precipitation stronger than 10mm in the neighbourhood (BSS_NO), considering spatial boxes of 76km.

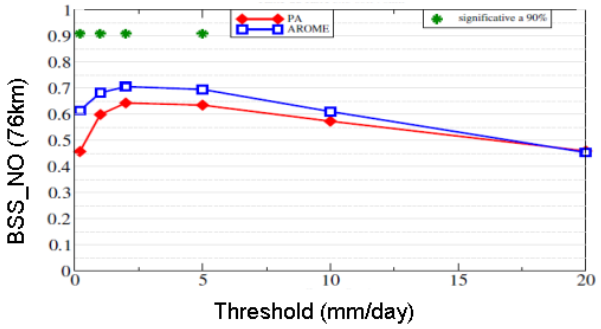

Figure 10: BSS_NO for summer 2012 for ARPEGE (in red) and AROME (in blue) according to the precipitation threshold (in mm/day)

The initialization of multimodal aerosols by MACC analysis (ECMWF) is on study. Parallely, the [Morrison and Grabowski, 2008]'s scheme, based on the novel approach that allows ice particle type to vary as a function of the rime and vapor deposition ice mixing ratios, is currently implemented in Meso-NH. Both schemes will be compared to the current 1-moment mixed scheme on heavy precipitating events of SOP1 of HYMEX experiment. This will give some basis for the future microphysical scheme of AROME.

6 Scores and test cases

The comparison of AROME and ARPEGE in a deterministic approach shows that on the monthly biases, AROME performs better than ARPEGE during summer, and it is the contrary during winter (Fig. 9). As the double penalty can disadvantage AROME, a fuzzy approach is addressed [Amodei and Stein, 2009]. The Brier Skill Score (BSS) against persistence with the size of the neighbourhood of 76 km indicates that AROME performs almost always better (a BSS of 1.0 indicates a perfect probability forecast). A zoom over last summer (Fig. 10) shows that ARPEGE forecasts too many weak precipitation events while it is partly corrected with AROME.

AROME has also run at 5km resolution over a large domain on the 23-28 July convective period of the AMMA 2006 field experiment [Beucher et al., 2013]. During this period, the convective activity

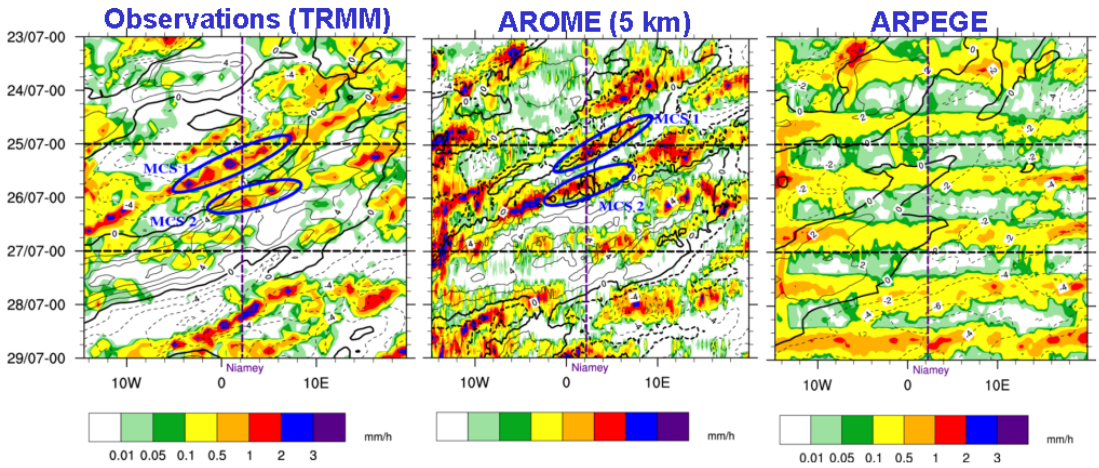

Figure 11: Hovmuller diagram of (a) the TRMM 3 h precipitation (mmh^{-1} ; colored areas) and the meridional wind at 700hPa (isocontours every 2$m.s^{-1}$ with a thick solid line for 0 ; solid and dashed lines for southerly and northerly winds respectively) for the 23-28 July period and averaged between 8N and 15N. The vertical line displays the longitude of Niamey. (b) Idem for AROME (5km resolution) 144-h forecast. (c) Idem for ARPEGE 144-h forecast. From [Beucher et al., 2013].

is characterized by westward fast-moving systems, with the passage over Niamey of two major events MCS1 and MCS2 (Fig. 11). The scenario proposed by the AROME forecast is in agreement with the observed one with similar African Easterly Waves (AEW) and moonsoon surge, associated with westward fast-moving MCSs. Only both simulated MCSs are slightly shifted to the south, pass at Niamey a few hours earlier and the diurnal convection is a bit too active. On the contrary ARPEGE cannot catch the modulation of precipitation by the AEW and by the moonsoon surge.

7 Conclusion

The AROME model, that is operational since 2008, has proved beneficial for forecasts over France, and is also embedded in the HARMONIE (Hirlam Aladin Research for Mesoscale Operational NWP In Europe) system. AROME forecasts often provide a good physical realism, which can be attributed to its mesoscale physics-dynamics and data assimilation scheme. The ARPEGE forecasts have been significatively improved these three last years, partly due to evolution in its physics, which tends to approach AROME's one (turbulence, shallow convection). But microphysics and cloud schemes keep some differences. For ARPEGE but also for AROME, subgrid cloud variability remains important. In AROME, the recent evolutions of the cloud scheme have improved cumuli and winter clouds representation, and the introduction of a double gaussian distribution could lead to an additional benefit for shallow cumuli and fractional stratocumuli. Also the introduction of subgrid rain would allow a gradual transition from non-precipitating to fully precipitating models grids. By 2014, thanks to a new supercomputer, the resolutions of AROME will be improved with 90 vertical levels and the lowest one at 5m instead of 10m currently, and an horizontal grid mesh of 1.3km over an extended domain. First tests in the new configuration over 3 months of summer 2012 show a reduction of overestimated rainfalls during afternoon, and we can expect a better representation of fog events with the finer low-level resolution. In the next step, the introduction of a 2-moment mixed microphysical scheme in AROME will be considered and for the moment, different options are studied in the research model Meso-NH.

References

[Amodei and Stein, 2009] Amodei, M. and Stein, J. (2009). Deterministic and fuzzy verification methods for a hierarchy of numerical models. *Meteorol. Appl.*, 16:191–203.

[Bechtold et al., 2001] Bechtold, P., Bazile, E., Guichard, F., Mascart, P., and Richard, E. (2001). A mass-flux convection scheme for regional and global models. *Quart. J. Roy. Meteor. Soc.*, 127:869–886.

[Bechtold et al., 1995] Bechtold, P., Cuijpers, J., Mascart, P., and Trouilhet, P. (1995). Modelling of trade-wind cumuli with a low-order turbulence model - toward a unified description of cu and sc clouds in meteorological models. *J. Atmos. Sci.*, 52:455–463.

[Beucher et al., 2013] Beucher, F., Lafore, J. P., and Karbou, F. (2013). The arome performance during the 2006 west african monsoon. To be submitted.

[Bougeault, 1982] Bougeault, P. (1982). Cloud-ensemble relations based on the gamma probability distribution for the higher-order models of the planetary boundary layer. *J. Atmos. Sci.*, 39:2691–2700.

[Bougeault, 1985] Bougeault, P. (1985). A simple parameterisation of the large scale effects of cumulus convection. *Mon. Wea. Rev.*, 4:469–485.

[Bougeault and Lacarrere, 1989] Bougeault, P. and Lacarrere, P. (1989). Parameterization of orography-induced turbulence in a meso-beta scale model. *Mon. Wea. Rev.*, 117:1870–1888.

[Bouteloup et al., 2005] Bouteloup, Y., Bouyssel, F., and Marquet, P. (2005). Improvments of lopez prognostic large scale cloud and precipitation scheme. *ALADIN Newsletter*, 28:66–73.

[Bouteloup et al., 2011] Bouteloup, Y., Seity, Y., and Bazile, E. (2011). Description of the sedimentation scheme used operationally in all Météo-France NWP models. *Tellus*, 63A:300–311.

[Caniaux et al., 1994] Caniaux, G., Redelsperger, J.-L., and Lafore, J.-P. (1994). A numerical study of the stratiform region of a fast-moving squall line. *J. Atmos. Sci.*, 51:2046–2074.

[Caumont et al., 2009] Caumont, O., Ducrocq, V., Wattrelot, E., Jaubert, G., and Pradier-Vabre, S. (2009). 1d+3dvar assimilation of radar reflectivity data: A proof of concept. *Tellus*, pages DOI :10.1111/j.1600–0870.2009.00430.x.

[Cuxart et al., 2000] Cuxart, J., Bougeault, P., and Redelsberger, J.-L. (2000). A turbulence scheme allowing for mesoscale and large-eddy simulations. *Quart. J. Roy. Meteor. Soc.*, 126:1–30.

[Ebert and Curry, 1992] Ebert, E. and Curry, J. A. (1992). A parameterization of ice cloud optical properties for climate models. *J. Geophys. Res.*, 97:3831–3835.

[F. Couvreux and Rio, 2010] F. Couvreux, F. H. and Rio, C. (2010). Resolved versus parametrized boundary-layer plumes. part i : A parametrization-oriented conditional sampling in large-eddy simulations. *Bound. Layer Meteor*, 134:441–458.

[Fouquart and Bonnel, 1980] Fouquart, Y. and Bonnel, B. (1980). Computations of solar heating of the earth s atmosphere: A new parameterization. *Beitr. Phys. Atmos.*, 53:35–62.

[Golaz et al., 2002a] Golaz, J., Larson, V. E., and Cotton, W. R. (2002a). A PDF-based parameterization for boundary layer clouds. Part I: Method and model description. *J. Atmos. Sci.*, 59:3540–3551.

[Golaz et al., 2002b] Golaz, J., Larson, V. E., and Cotton, W. R. (2002b). A PDF-based parameterization for boundary layer clouds. Part II: Model results. *J. Atmos. Sci.*, 59:3552–3571.

[Lafore et al., 1998] Lafore, J.-P., Stein, J., Asencio, N., Bougeault, P., Ducrocq, V., Duron, J., Fischer, C., Hereil, P., Mascart, P., Masson, V., Pinty, J.-P., Redelsperger, J. L., Richard, E., and de Arellano, J. V.-G. (1998). The meso-nh atmospheric simulation system. part i: adiabatic formulation and control simulations. *Annales Geophysicae*, 16:90–109.

[Larson et al., 2001a] Larson, V. E., Wood, R., Field, P. R., Golaz, J., VonderHaar, T. H., and Cotton, W. R. (2001a). Small-scale and mesoscale variability of scalars in cloudy boundary layers: One dimensional probability density functions. *J. Atmos. Sci.*, 58:1978–1994.

[Larson et al., 2001b] Larson, V. E., Wood, R., Field, P. R., Golaz, J.-C., VonderHaar, T. H., and Cotton, W. R. (2001b). Systematic biases in the microphysics and thermodynamics of numerical models that ignore subgrid-scale variability. *J. Atmos. Sci.*, 58:1117–1128.

[Lascaux et al., 2006] Lascaux, F., Richard, E., and Pinty, J.-P. (2006). Numerical simulations of three MAP IOPs and the associated microphysical processes. *Quart. J. Roy. Meteor. Soc.*, 132:1907–1926.

[Lenderink and Siebesma, 2000] Lenderink, G. and Siebesma, P. (2000). Combining the mass-fluw approach with a statistical cloud scheme. In *Proceedings of 14th Symposium on boundary layers and turbulence*, Aspen, USA.

[Lin et al., 1983] Lin, Y. L., Farley, R. D., and Orville, H. D. (1983). Bulk parameterization of the snow field in a cloud model. *Journal of Climate and Applied Meteorology*, 22:1065–1092.

[Lopez, 2002] Lopez, P. (2002). Implementation and validation of a new prognostic large-scale cloud and precipitation scheme for climate and data-assimilation purposes. *Quart. J. Roy. Meteor. Soc.*, 128:229–257.

[Martin et al., 1994] Martin, G. M., Johnson, D. W., and Spice, A. (1994). The measurement and parameterization of effective radius of droplets in warm stratocumulus. *J. Atmos. Sci.*, 51:1823–1842.

[Mlawer et al., 1997] Mlawer, E. J., Taubman, S. J., Brown, P., Iacono, M. J., and Clough, S. A. (1997). Radiative transfer for inhomogeneous atmospheres: Rrtm, a validated correlated-k model for the longwave. *J. Geophys. Res.*, 102:16663–16682.

[Montmerle and Faccani, 2009] Montmerle, T. and Faccani, C. (2009). mesoscale assimilation of radial velocities from doppler radars in a preoperational framework. *Mon. Wea. Rev.*, 137:1939–1953.

[Morcrette and Fouquart, 1986] Morcrette, J.-J. and Fouquart, Y. (1986). The overlapping of cloud layers in shortwave radiation parameterizations. *J. Atmos. Sci.*, 43:321–328.

[Morrison and Grabowski, 2008] Morrison, H. and Grabowski, W. W. (2008). A novel approach for representing ice microphysics in models: Description and tests using a kinematic framework. *J. Atmos. Sci.*, 65:1528–1548.

[Ou and Liou, 1995] Ou, S. C. and Liou, K.-N. (1995). Ice microphysics and climatic temperature feedback. *Atmos. Res.*, 35:127–138.

[Pergaud et al., 2009] Pergaud, J., Masson, V., Malardel, S., and Couvreux, F. (2009). A parameterization of dry thermals and shallow cumuli for mesoscale numerical weather prediction. *Bound.-Layer Meteor.*, 132:83–106.

[Perraud et al., 2011] Perraud, E., Couvreux, F., Malardel, S., Lac, C., Masson, V., and Thouron, O. (2011). Evaluation of statistical distributions for the parametrization of subgrid boundary-layer clouds. *Bound.-Layer Meteor.*, 140:263–294.

[Pruppacher and Klett, 1978] Pruppacher, H. R. and Klett, J. D. (1978). *Microphysics of clouds and precipitation.* D. Reidel Publishing Company. 714pp.

[Rooy et al., 2010] Rooy, W. D., Bruijn, C. D., Tijm, S., Neggers, R., Siebesma, P., and Barkmeijer, J. (2010). Experiences with Harmonie at KNMI. *HIRLAM Newsletter*, 56:21–29.

[S. Berthet, 2010] S. Berthet, J-P. Pinty, M. L. (2010). Treatment of multiple size-distributed populations of ccn and ifn in a 2-moment microphysical scheme of the cloud-resolving model mesonh. In *European Geosciences Union*, Vienna, Austria.

[Seity et al., 2010] Seity, Y., Brousseau, P., Malardel, S., Hello, G., Bénard, P., Bouttier, F., Lac, C., and Masson, V. (2010). The AROME-France convective-scale operational model. *Mon. Wea. Rev.*, 139:976–991.

[Smith, 1990] Smith, R. N. B. (1990). scheme for predicting layer clouds and their water content in a general circulation model. *Quart. J. Roy. Meteor. Soc.*, 116:435–460.

[Turner et al., 2012] Turner, S., Brenguier, J.-L., and Lac, C. (2012). A subgrid parameterization scheme for precipitation. *Geoscientific Model Development*, 5(2):499–521.

[Wattrelot et al., 2008] Wattrelot, E., Caumont, O., Pradier-Vabre, S., Jurasek, M., and Haase, G. (2008). 1D + 3DVar assimilation of radar reflectivities in the pre-operational AROME model at Meteo-France. In *Fifth Conf. on radar in Meteorology and Hydrology*, Helsinki, Finland. Finnish Meteorological Institute.